

Calculation of spectral peaks in a chaotic dc–dc converter

J.H.B. Deane, P. Ashwin*, D.C. Hamill and D.J. Jefferies

School of Electronic Engineering, Information Technology and Mathematics,
University of Surrey,
Guildford GU2 5XH,
United Kingdom

Abstract

A simple mapping is derived which describes the behaviour of a peak current-mode controlled boost converter operating chaotically. The invariant density of this mapping is calculated iteratively, and from this the power spectral density of the input current at the clock frequency and its harmonics is deduced. The calculation is presented, along with experimental verification, and the possibility of EMC improvement by chaos is discussed.

1. Introduction

In a previous publication [1] we presented the idea that chaos, a naturally occurring phenomenon in switch-mode power supplies, might be used to improve their electromagnetic compatibility. We illustrated this proposal with some measurements. In the present paper we show how to calculate the power spectral density (PSD) at the clock frequency and its harmonics, of the input current of a current-mode controlled boost converter operating chaotically. This work builds mainly on [2]–[4], in which we derived an exact two-dimensional mapping in closed form that describes the behaviour of this converter. The requirement for low output voltage ripple in practical designs leads to a circuit that is well described by a simpler one-dimensional mapping, derived in this paper. We show how to calculate its invariant density, and then use this to calculate the PSD of the inductor current. We then confirm experimentally and numerically the validity of the model and our PSD calculation. We also discuss briefly the implications for EMC improvement by chaos.

2. The simplified mapping

A two-dimensional mapping that describes the boost converter in figure 1 was presented in [1]; another two-dimensional version, taking into account inductor and capacitor parasitics, appears in [5].

The mapping that describes a boost converter as usually designed, however, can be simplified to a one-dimensional version that nonetheless captures the features of interest in the behaviour of the real circuit. In order to derive this one-dimensional mapping, we make the following assumptions:

*Partially supported by the Nuffield Foundation via a ‘Newly appointed science lecturer’ grant.

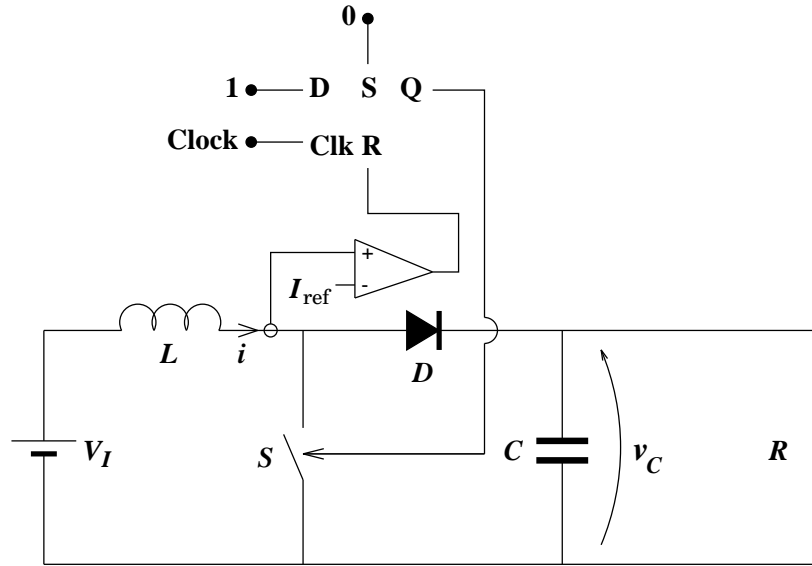


Figure 1: The peak current-mode controlled boost converter.

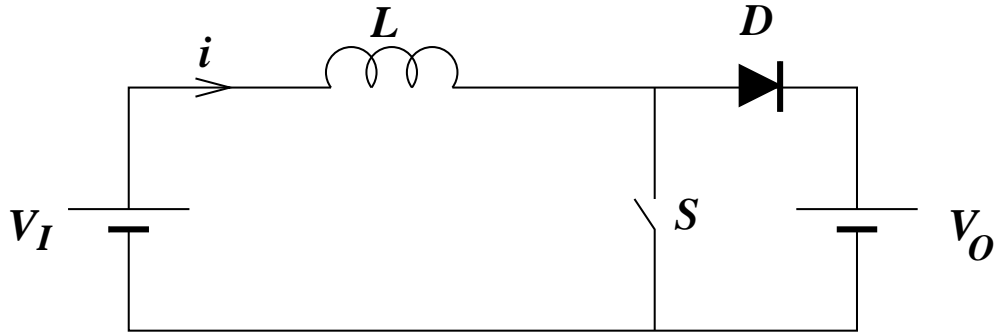


Figure 2: Simplified model of the power circuit of the boost converter.

1. The output voltage is sufficiently close to a constant, \bar{V}_O that the inductor current waveform can be approximated by a linear ramp at all times. This requires that $CR \gg T$, where T is the clock period. In practical circuits, C is sufficiently large for this to be valid.
2. All components are ideal.
3. The clock pulses are of infinitesimal duration and period T .

With these assumptions, the power circuit can be modelled in the simplified form shown in figure 2. The switch S is controlled by feedback. It closes when a clock pulse arrives and opens at the instant when $i(t)$ reaches the reference current I_{ref} .

The inductor current $i(t)$ is sketched in figure 3. While S is closed, $i(t)$ satisfies

$$\frac{di}{dt} = \frac{V_I}{L}$$

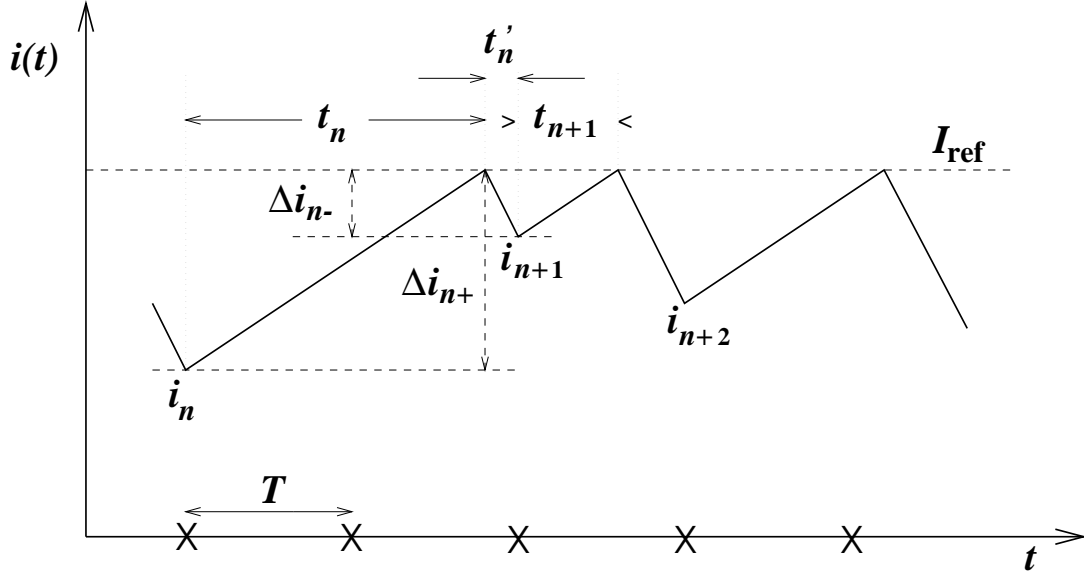


Figure 3: The current waveform $i(t)$ in the simplified boost converter.

If $t = 0$ at the instant of S closing, then $i(t)$ is

$$i(t) = i_n + \frac{V_I}{L}t \quad (1)$$

valid until time t_n at which $i(t_n) = I_{\text{ref}}$. Using equation (1)

$$t_n = \frac{(I_{\text{ref}} - i_n)L}{V_I} \quad (2)$$

Switch S now opens and $i(t)$ is given by

$$\frac{di}{dt} = \frac{V_I - \bar{V}_O}{L}$$

with initial condition $i(0) = I_{\text{ref}}$. (We reset the time origin for convenience.) Hence,

$$i(t) = I_{\text{ref}} + \frac{V_I - \bar{V}_O}{L}t \quad (3)$$

until the next clock pulse arrives. This happens at a time

$$t'_n = T - T \left(\frac{t_n}{T} \right) \bmod 1 \quad (4)$$

after S last opened.

The mapping $i_n \mapsto i_{n+1}$ can now be derived. By definition, $i_{n+1} = i(t'_n)$, which according to equations (2), (3) and (4), is

$$i_{n+1} = I_{\text{ref}} + \frac{(V_I - \bar{V}_O)T}{L} \left[1 - \left(\frac{(I_{\text{ref}} - i_n)L}{V_I T} \right) \bmod 1 \right] \quad (5)$$

Introducing a dimensionless time x_n , defined as

$$x_n = \frac{t_n}{T} = \frac{(I_{\text{ref}} - i_n)L}{V_I T}$$

and parameter α , defined as

$$\alpha = \frac{\bar{V}_O}{V_I} - 1$$

the mapping (5) can be written in the simplified form

$$x_{n+1} = F(x_n) = \alpha(1 - x_n \bmod 1) \quad (6)$$

Since $\bar{V}_O > V_I$ for a boost converter, $\alpha > 0$.

Note that the switching times can be recovered from (6):

$$t_n = T x_n \quad \text{and} \quad t'_n = T(1 - x_n \bmod 1) \quad (7)$$

This map and scaled versions of it have been studied in several contexts, most notably by Rényi [6] and [7, section 6.2]. The fact that F is the Rényi transformation means that the Perron-Frobenius operator P , defined in the Appendix, has an invariant density $\rho(x)$ that is ergodic and asymptotically stable [7, Theorem 6.2.1]. This density is calculated in the Appendix.

3. Approximation of the mean state variables

In order to use the mapping (6), we need to know the value of α , and hence there remains the problem of relating \bar{V}_O , the mean output voltage, to known quantities in the circuit. We obtain an estimate of \bar{V}_O by assuming that S is closed on average for a time $\bar{D}T$ per clock cycle; and \bar{V}_O is constant. Here, \bar{D} is to be interpreted as the mean duty factor of S . On average,

$$\bar{V}_O = R(1 - \bar{D}) \left(I_{\text{ref}} - \frac{\bar{\Delta}i}{2} \right) \quad (8)$$

where R is the load resistance shown in figure 1. This assumes that the current through the diode is either zero (for a fraction \bar{D} of the time) or $I_{\text{ref}} - \bar{\Delta}i/2$ (for a fraction $1 - \bar{D}$ of the time). When S is closed, i rises at a rate of V_I/L for a time $\bar{D}T$ on average; when S is open, i falls at a rate $(\bar{V}_O - V_I)/L$ for a time $(1 - \bar{D})T$. In terms of the mean current rise, $\bar{\Delta}i_+$, and fall, $\bar{\Delta}i_-$,

$$\bar{\Delta}i_+ = \frac{V_I}{L} \bar{D}T, \quad \bar{\Delta}i_- = \frac{\bar{V}_O - V_I}{L} (1 - \bar{D})T \quad \text{and} \quad \bar{\Delta}i_+ = \bar{\Delta}i_- = \bar{\Delta}i \quad (9)$$

Eliminating $\bar{\Delta}i_+$, $\bar{\Delta}i_-$, $\bar{\Delta}i$ and \bar{D} between equations 8 and 9, gives

$$\bar{V}_O^3 + \bar{V}_O(V_I T/2L - I_{\text{ref}})RV_I - RTV_I^3/2L = 0 \quad (10)$$

which can be solved for \bar{V}_O by selecting the real root $\bar{V}_O > V_I$. Hence, α can be found.

4. The power spectral density of the inductor current

We use properties of the mapping $x_{n+1} = F(x_n)$ to compute the PSD of the current through the inductor, $i(t)$. This splits into two cases: chaotic and periodic.

Recall that the power spectral density is the generalised Fourier transform of the autocorrelation function

$$R_i(\tau) = \lim_{T \rightarrow \infty} \frac{1}{T} \int_0^T i(t)i(t+\tau) dt$$

and write the PSD as $\tilde{I}(\omega)$.

4.1 Chaotic case

When $\alpha > 1$, the sequence $\{x_0, x_1, \dots, x_n \dots\}$ will be chaotic with each x_n lying between 0 and α ; more precisely the transformation has an ergodic invariant measure with density ρ that is absolutely continuous with respect to Lebesgue measure on the interval $[0, \alpha)$.

We claim that $\tilde{I}(\omega)$ is a sum of two functions, namely a sum of δ -functions at harmonics of the clock frequency and a continuous function that corresponds to broadband noise. Specifically, we claim that there are no δ -function peaks except those at the harmonics of the clock frequency, which seems to be reasonable, since chaos is an aperiodic phenomenon.

Under assumption (1) of section 2., d^2i/dt^2 is a sequence of Dirac δ -functions of alternating sign and amplitude \bar{V}_O/L . The integration property of Fourier transforms

$$v(t) \Leftrightarrow V(\omega) \quad \Longrightarrow \quad \int_{-\infty}^t v(u) du \Leftrightarrow \frac{1}{j\omega} V(\omega)$$

applied twice, allows us to recover spectral properties of $i(t)$ rather than its second derivative. Throughout this section we use the dimensionless time $x = t/T$. The situation is then as illustrated in figure 4.

Using the time shift property of Fourier transforms, $v(t) \Leftrightarrow V(\omega) \Longrightarrow v(t - \tau) \Leftrightarrow e^{-j\omega\tau} V(\omega)$, and the fact that $\delta(t) \Leftrightarrow 1$, we define

$$I_N(\omega) = -\frac{1}{\omega^2} \frac{\bar{V}_O}{L} \frac{1}{N} [\{1 - \exp(-j\omega T x_1)\} + \exp(-j\omega T [1 + \lfloor x_1 \rfloor]) \{1 - \exp(-j\omega T x_2)\} + \dots \\ + \exp(-j\omega T [N - 1 + \lfloor x_1 \rfloor + \dots + \lfloor x_{N-1} \rfloor]) \{1 - \exp(-j\omega T x_N)\}] \quad (11)$$

where $\lfloor x \rfloor = x \bmod 1$ is the integer part of x ; the factor $-1/\omega^2$ represents twice integrating; and the factor \bar{V}_O/L , which is the difference between di/dt when the switch is closed and when it is open, sets the vertical scale correctly. Defining the integers J_n as

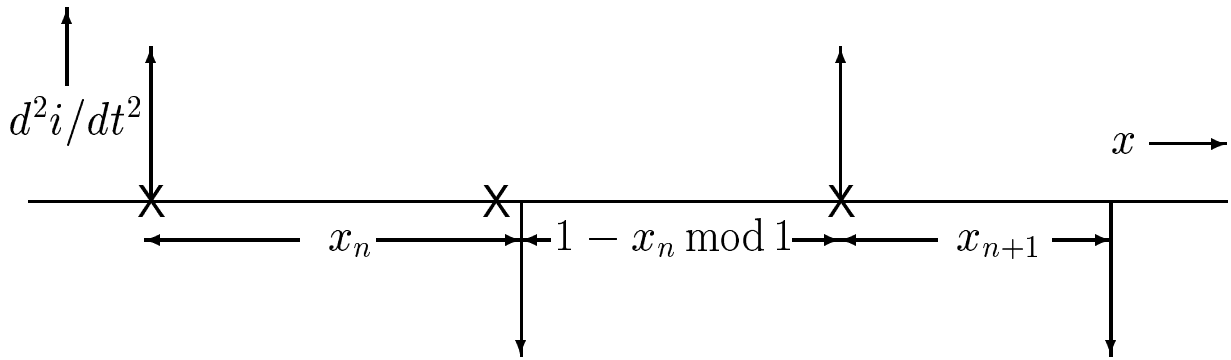


Figure 4: The second derivative of the current waveform. The vertical arrows represent δ -functions of amplitude $\pm\bar{V}_O/L$ and the clock pulses are represented by X.

$$J_n = \begin{cases} 0 & n = 1 \\ \sum_{k=1}^{n-1} 1 + [x_k] = n - 1 + \sum_{k=1}^{n-1} [x_k] & n > 1 \end{cases}$$

equation (11) can be rewritten

$$I(\omega) = \lim_{N \rightarrow \infty} I_N(\omega) = -\frac{\bar{V}_O}{\omega^2 L} \lim_{N \rightarrow \infty} \frac{1}{N} \sum_{n=1}^N e^{-j\omega T J_n} \{1 - e^{-j\omega T x_n}\} \quad (12)$$

‘Brute force’ calculations of the PSD can be carried out by summing this series for some large N . The expression simplifies when ω corresponds to the clock frequency, ω_c , or its harmonics. For the m -th harmonic, $\omega = m\omega_c = m \cdot 2\pi/T$, and so equation (12) becomes

$$I(m\omega_c) = -\frac{\bar{V}_O}{m^2 \omega_c^2 L} \lim_{N \rightarrow \infty} \frac{1}{N} \sum_{n=1}^N 1 - e^{-2j\pi m x_n} \quad (13)$$

This sum can be evaluated by using ergodicity of ρ and Birkhoff’s Ergodic Theorem [9]. Given an expanding map F which preserves the ergodic measure with density $\rho(x)$ on $[0, \alpha)$:

$$\lim_{N \rightarrow \infty} \frac{1}{N} \sum_{n=1}^N \phi(F^{[n-1]}(x)) = \int_0^\alpha \phi(y) \rho(y) dy \quad (14)$$

for (Lebesgue) almost all initial conditions x and for any continuous function ϕ which maps $[0, \alpha)$ to \mathcal{R} . Here, $F^{[i]}(x)$ is the i -th iterate of F .

In order to evaluate the integral in equation (14), we therefore need to calculate the invariant density of F , $\rho(x)$, which is the normalised density of iterates $\{x_0, x_1, \dots\}$ of the mapping, over the interval $[0, \alpha)$. In terms of $\rho(x)$, $I(m\omega_c)$ is given by

$$I(m\omega_c) = -\frac{\bar{V}_O}{m^2 \omega_c^2 L} \int_0^\alpha (1 - e^{-j2\pi m x}) \rho(x) dx = \frac{\bar{V}_O}{m^2 \omega_c^2 L} \left[\int_0^\alpha e^{-j2\pi m x} \rho(x) dx - 1 \right] \quad (15)$$

where the second equality follows from the fact that $\rho(x)$ is normalised. Finally, we can use a result in Champeney [8, Theorem 11.10] to note that $\tilde{I}(\omega)$ must therefore have a δ -function with height given by $|I(m\omega_c)|^2$ at $\omega = m\omega_c$.

4.2 Periodic case

It is now interesting to compare chaotic and periodic operation of the boost converter under the same conditions, *i.e.* with the same \bar{V}_O in both cases. Experimentally, this can be achieved by removing the feedback loop in figure 1 and instead driving the switch periodically, using a pulse generator, such that the output voltage is the same as in the chaotic case.

Taking equation (12) as our starting point, in the periodic case this becomes

$$I_p(\omega) = -\frac{\bar{V}_O}{\omega^2 L} \lim_{N \rightarrow \infty} \frac{1}{N} \sum_{n=1}^N e^{-j\omega n T} (1 - e^{-j\omega \bar{D} T}) \quad (16)$$

where \bar{D} can be calculated by eliminating $\bar{\Delta i}$ between equations (8) and (9). When $\omega \neq m\omega_c$ for integer $m \geq 1$, this sums to zero. To find $I_p(m\omega_c)$ we calculate

$$I_p(m\omega_c) = -\frac{\bar{V}_O}{m^2 \omega_c^2 L} (1 - e^{-jm\omega_c \bar{D} T}) \lim_{N \rightarrow \infty} \lim_{\delta \rightarrow 0} \frac{1}{N} \sum_{n=1}^N e^{-jmn(2\pi + \delta)} = -\frac{\bar{V}_O}{m^2 \omega_c^2 L} (1 - e^{-jm\omega_c \bar{D} T}) \quad (17)$$

Hence

$$|I_p(m\omega_c)| = \frac{\bar{V}_O}{m^2 \omega_c^2 L} \sqrt{2(1 - \cos 2m\pi \bar{D})} \quad (18)$$

5. Results

Twenty iterations of the Perron-Frobenius operator (see Appendix) give the approximation to $\rho(x)$ for $\alpha = 2.65$ shown in figure 5.

Using the invariant density and equation (15) we can calculate the PSD as explained in the previous section. It is also possible, although computationally inefficient, to estimate this by brute force — equation (13) — and for the purposes of comparison, this was also carried out for $N \approx 2000$. The results, which are in excellent agreement with each other, are displayed in figure 6, along with the PSD obtained from experiment.

It is interesting to note how the PSD at a given harmonic of the clock frequency varies with α , and this is displayed in figures 7(a) and (b) for the first, second, fifth and tenth harmonics. For a comparison of chaotic with periodic operation, see figure 8. This shows how the calculated spectral peaks at ω_c , $2\omega_c$, $5\omega_c$ and $10\omega_c$ vary with α , when the converter is allowed to operate chaotically, and when it is forced to operate periodically, \bar{V}_O being the same in each case. Experimental results on this were published in [1]. It can be seen from figure 8 that for the first and second harmonics, the PSD is always less in the chaotic case, but that this is not necessarily so for the other harmonics considered.

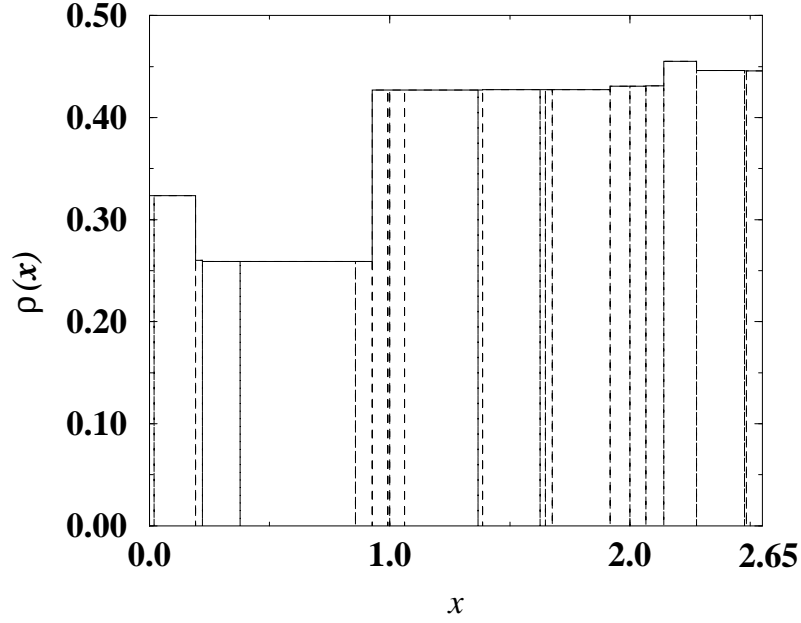


Figure 5: The invariant density for $\alpha = 2.65$. The dotted lines show the partitions.

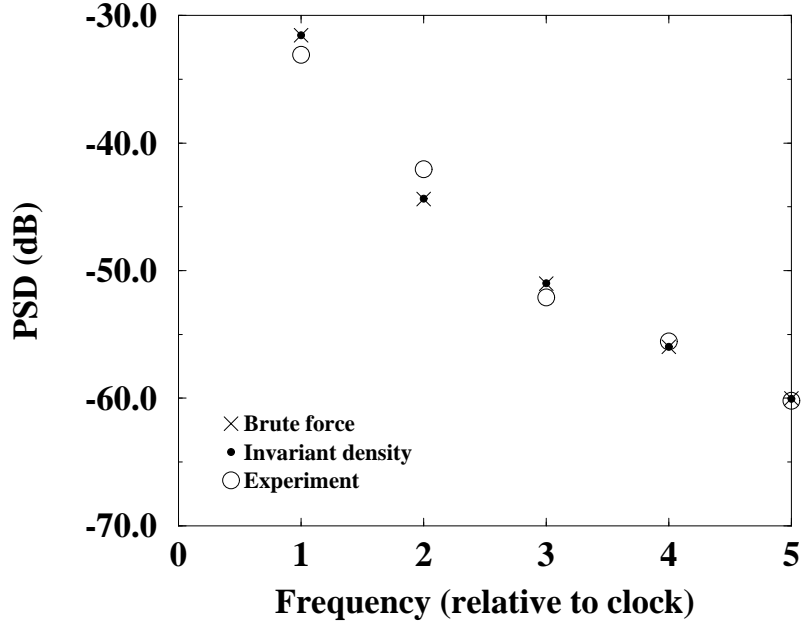


Figure 6: Three-way comparison of the inductor current PSD at the clock frequency and its harmonics, by brute force (equation 13), the invariant density method, and experiment. The scaling factor of $\overline{V_O T^2}/L$ has been taken as unity and $\alpha = 2.65$.

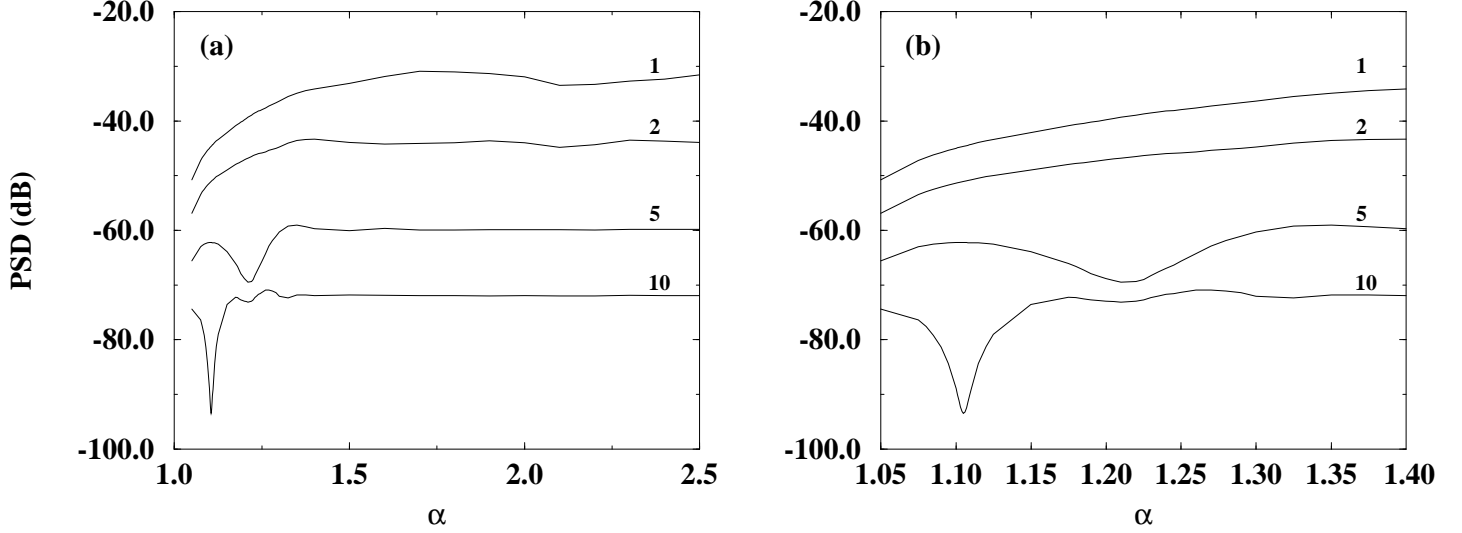


Figure 7: (a) The PSD at ω_c , $2\omega_c$, $5\omega_c$ and $10\omega_c$ as a function of α . (b) As (a), but on an expanded scale.

6. Experimental results

The peak-current controlled boost converter shown in figure 1 was built, using $R = 293\Omega$, $L = 104\text{mH}$, $C = 220\mu\text{F}$, $V_I = 10.45\text{V}$, $\bar{V}_O = 32.3\text{V}$, reference current $I_{\text{ref}} = 0.5\text{A}$ and clock period $T = 400\mu\text{s}$. The total inductor series resistance $r_L = (1.0 + 2.33)\Omega$, the 1Ω being a current sensing resistor. With these parameter values the circuit behaved chaotically. The output voltage had a chaotic ripple of peak to peak amplitude $\approx 0.6\text{V}$.

An analogue-to-digital converter was used to monitor the inductor current $i(t)$. A section of the experimental current waveform, sampled at 40kHz , is shown in figure 9. An experimental version of the mapping given in equation (6) was reconstructed from the turning points of a rather longer portion of this waveform, and is shown in figure 10. The shape is exactly that expected from the theoretical mapping, equation (6), confirming that the one-dimensional approximation is appropriate. The value of α that applies to this converter can be arrived at in several ways. These include:

1. By definition, $\alpha = \text{Effective}(\bar{V}_O/V_I) - 1$. The actual value of V_I was $10.45 \pm 0.06\text{V}$. The mean voltage drop across r_L was measured as $1.4 \pm 0.06\text{V}$, and hence the effective $V_I = 9.05 \pm 0.12\text{V}$. The measured value of \bar{V}_O was $32.3 \pm 0.26\text{V}$ and the drop across the diode was $0.8 \pm 0.1\text{V}$; hence the effective $\bar{V}_O = 33.1 \pm 0.36\text{V}$.

These results give $\alpha = 2.66 \pm 0.09$.

2. The gradients, with standard errors, of the three negative slope portions of the experimental mapping in figure 10 were found by least squares fit, giving a second experimental estimate of $\alpha = 2.66 \pm 0.02$.
3. Equation (10), derived from an approximate model of the circuit neglecting parasitic resistances,

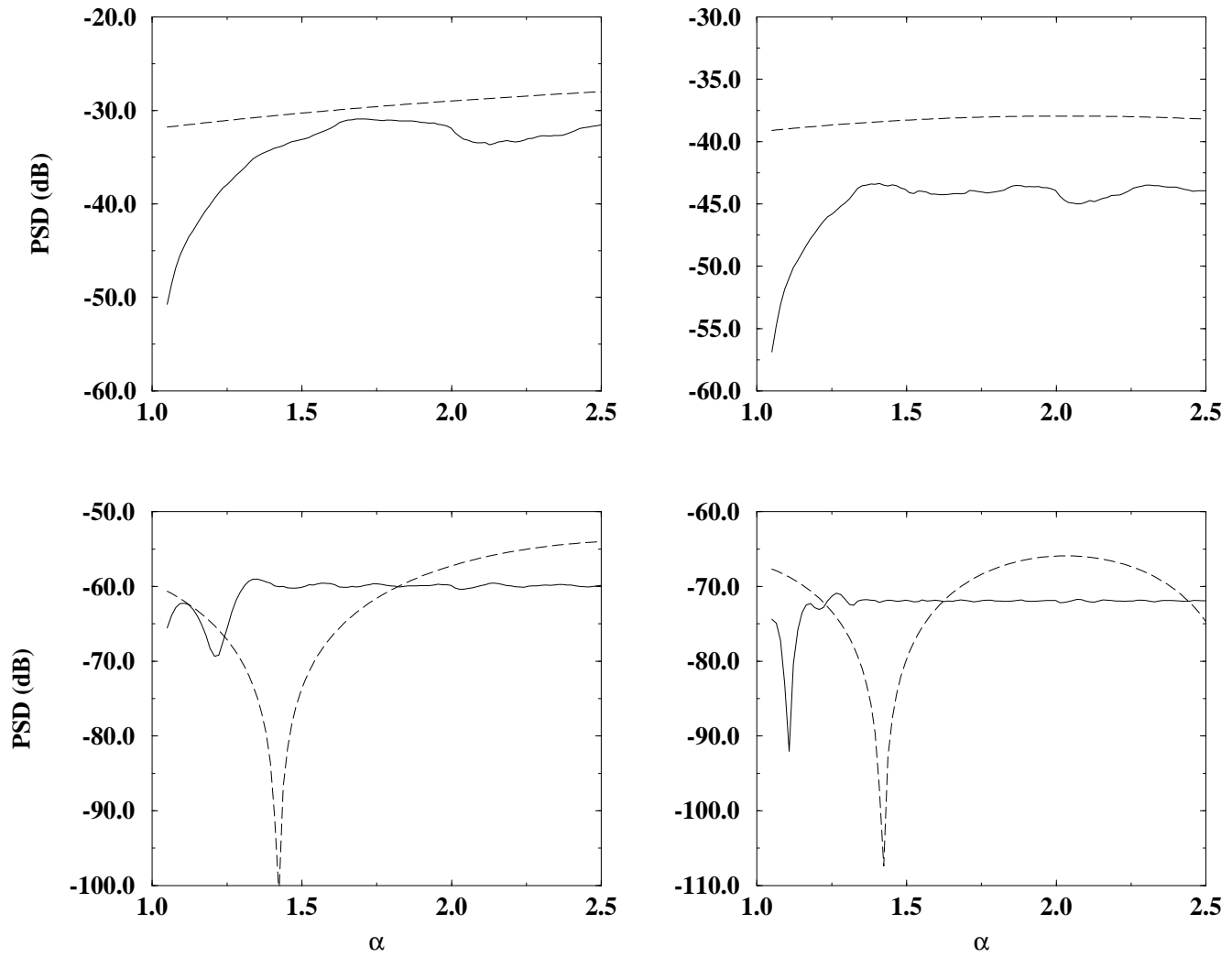


Figure 8: A comparison of chaotic and periodic operation. The PSD at ω_c (top left), $2\omega_c$ (top right), $5\omega_c$ (bottom left) and $10\omega_c$ (bottom right) is shown, as a function of α . Chaotic: continuous line; periodic: dashed line.

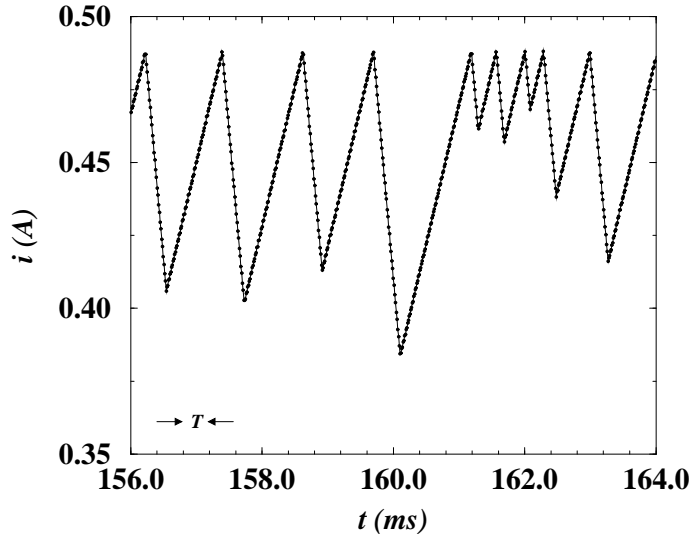


Figure 9: Experimental chaotic current waveform.

has the three roots $\bar{V}_O = -35.4, -0.32$ and $35.7V$, the first two of which can be rejected since they are negative. This gives $\alpha = 2.94$.

Finally, the FFT of a time series consisting of 2^{16} experimental samples of $i(t)$ was calculated and the result is shown in figure 11, along with a brute force calculation (equation 12). It can be seen that there is a good measure of agreement between the experiment and the calculation.

7. Discussion

The simplified one-dimensional mapping is adequate for practical versions of a chaotically operating boost converter. The power spectral density of the input current can be calculated from this sawtooth map, confirming an assertion we made in [11], that ‘the parameters at which subharmonics and chaos commence can be predicted accurately, as can ...the frequencies emitted from the power supply’. Measurements verify the accuracy of our calculations, which may therefore be used with confidence as a design tool in the specification of boost converter circuits where the EMC targets are tightly controlled. One important application is in high power-factor single-phase rectifiers for mains power supplies, *e.g.* [12].

A recent publication [13] sets out the conditions for the existence of *robust chaos*, which is characterised by the absence of periodic windows and co-existing attractors in some region of parameter space. The boost converter described here satisfies these conditions, guaranteeing chaotic operation. Although the full circuit description results in a two-dimensional mapping, we believe that the practical benefits of extending the analysis to this case are minimal, particularly in view of the extra theoretical and computational difficulties this would raise. There could, however, be an advantage in examining the sensitivity of the spectrum to the ‘nearly one-dimensional’ approximation, and this may form the basis for future investigations.

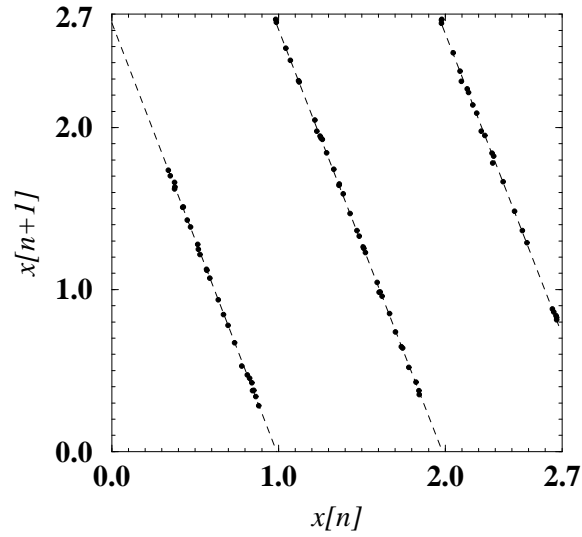


Figure 10: Experimental mapping deduced from the measured waveform; *cf.* equation 6. The dotted lines are a least squares fit to each of the linear portions of the mapping.

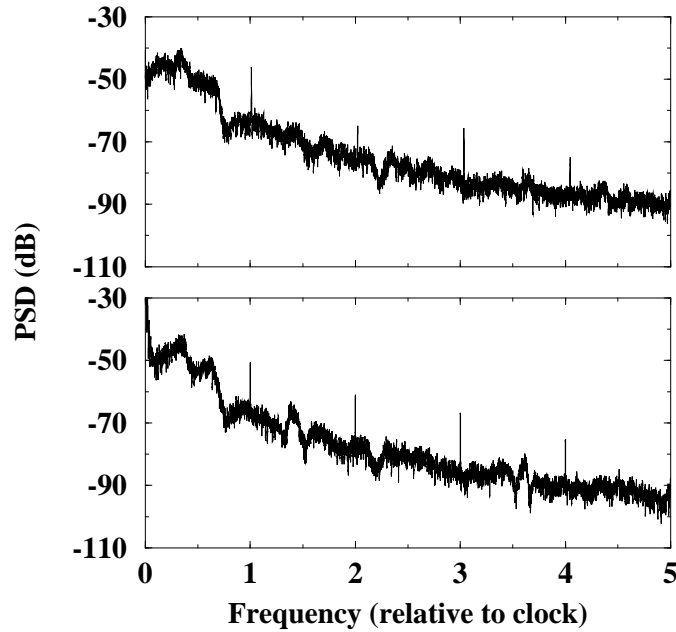


Figure 11: Experimental (top) and brute force calculation (bottom) of the PSD of $i(t)$ for $\alpha = 2.65$. Both spectra have been subjected to a 10-point running average.

Another extension of this work would involve calculating the PSD at frequencies other than the clock frequency and its harmonics. We believe this to be feasible.

Our results may, of course, be applied to other physical systems that can be described by a piecewise-linear one-dimensional mapping.

8. Conclusion

We have shown that spectral peaks of the input current in a boost converter in chaotic operation can be calculated. The predictions are in satisfactory agreement with measurements on a practical circuit. The calculation method may therefore be adopted by engineers for design purposes.

Appendix

The Perron-Frobenius operator P related to the mapping F , equation (6), is defined by

$$P(g)(x) = \sum_{y=F^{-1}(x)} \frac{1}{|F'(y)|} g(y)$$

Its invariant density, $\rho(x)$ can be calculated as the limit $\lim_{n \rightarrow \infty} \rho_n(x)$ where $\rho_n(x) = P(\rho_{n-1})(x)$, with $\rho_0(x)$ any non-negative function with integral one (*e.g.* a constant). This is illustrated in figure 12, in which $\alpha = 2.3$, but the scheme converges for any $\alpha > 1$.

The obvious choice for $\rho_0(x)$ is therefore

$$\rho_0(x) = \begin{cases} \frac{1}{\alpha} & 0 \leq x < \alpha \\ 0 & \text{otherwise} \end{cases}$$

which is clearly normalised. The x -axis is split into three intervals, labelled a , $[0, 1)$; b , $[1, 2)$; and c , $[2, \alpha]$. The densities on a and b are mapped by F uniformly and with equal weighting¹ onto a' and b' , where $a' = b' = [0, \alpha]$, but the density on c is mapped onto $c' = [\alpha, F(\alpha)] = [2.3, 1.61]$. The first approximation to ρ , $\rho_1(x)$ then comprises the sum of these three densities. To calculate ρ_2 from ρ_1 , the same procedure is used, except that this time there are eight sub-intervals to be considered, $a_1, a_2, b_1 \dots b_3$ and $c_1 \dots c_3$. All the intervals except $b_3 = [1.61, 2)$ have been treated before, and are dealt with in the same way again; b_3 is mapped to $b'_3 = [0, F^{[2]}(\alpha)] = [0, 0.897]$. The sum of these eight densities gives ρ_2 .

A computer program was written to iterate the Perron-Frobenius operator n times and plot the result. Note that this algorithm does not require the mapping $F(x)$ to have a finite number of Markov partitions [10]. It can also be modified to calculate the invariant densities of any piecewise-linear map, provided that the densities on each interval are mapped with a weighting factor equal to the modulus of the reciprocal of the gradient of the map in each interval.

¹This is because $|dF/dx| = \alpha$ everywhere except at $x = 1, 2, \dots$

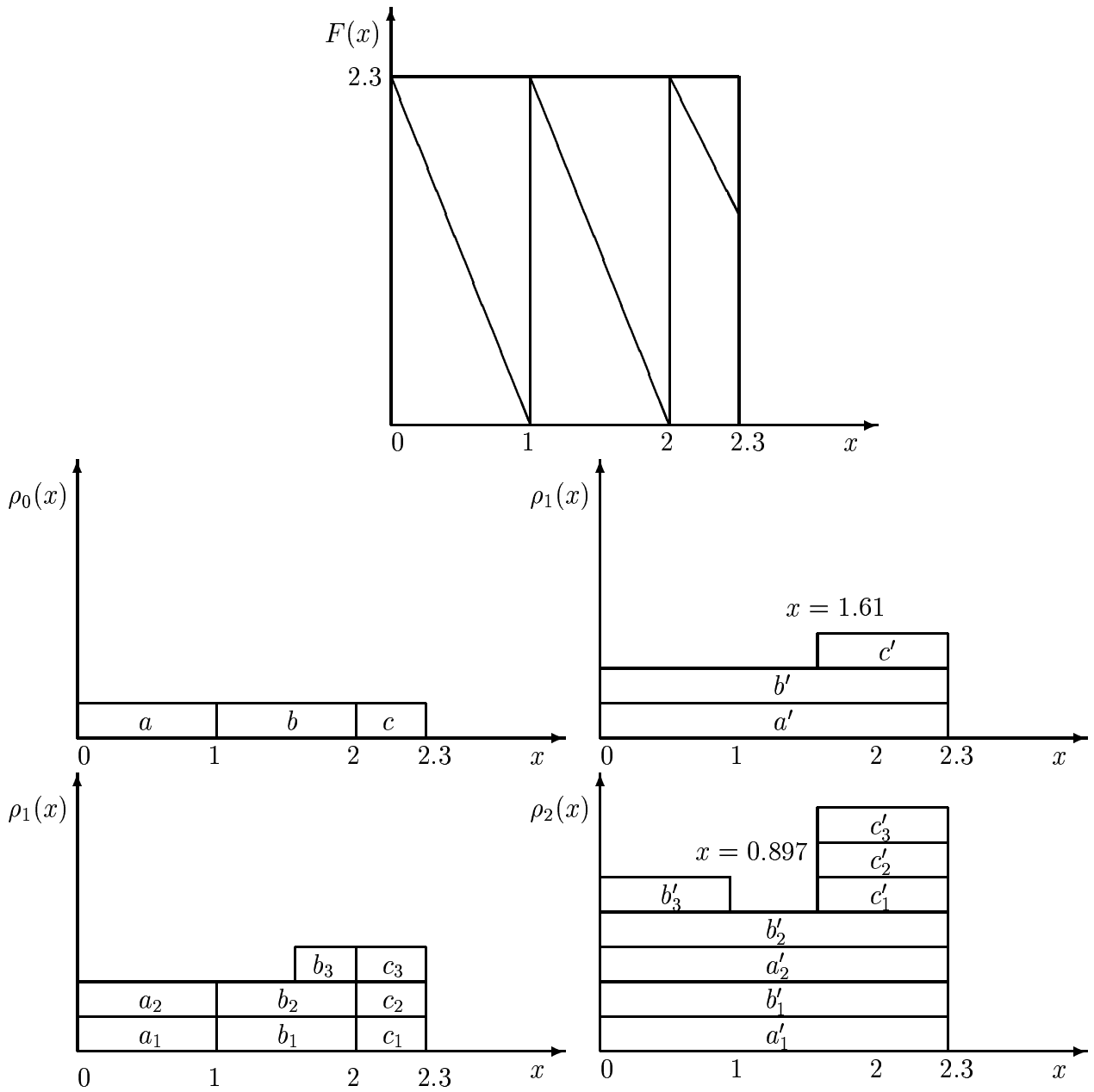


Figure 12: The map $F(x)$ and the algorithm for calculating the invariant density $\rho(x)$ by successive approximations $\rho_0, \rho_1, \rho_2, \dots$, with $\alpha = 2.3$.

References

- [1] J.H.B. Deane and D.C. Hamill, *Improvement of power supply EMC by chaos*, **Electronics Letters**, vol. 32 no. 12, page 1045 (June 1996)
- [2] J.H.B. Deane, *Chaos in a current-mode controlled boost dc-dc converter*, **IEEE Transactions on Circuits and Systems**, vol. 39 no. 8, pp 680–683 (August 1992)
- [3] D.C. Hamill, J.H.B. Deane and D.J. Jefferies, *Modelling of chaotic DC-DC converters by iterated non-linear mappings*, **IEEE Transactions on Power Electronics**, vol. PE-7, no. 1, pp 25–36 (January 1992)
- [4] J.H.B. Deane and D.C. Hamill, *Instability, subharmonics and chaos in power electronic systems*, **IEEE Transactions on Power Electronics**, vol. 5, no. 3, pp 260–268 (1990)
- [5] S. Banerjee and K. Chakrabarty, *Nonlinear Modeling and Bifurcations in the Boost Converter*, **IEEE Transactions on Power Electronics**, (March 1998, to appear)
- [6] A. Rényi, *Representation for real numbers and their ergodic properties*, **Acta Math. Acad. Sci. Hung.**, vol. 8, pp 477–493 (1957)
- [7] A. Lasota and M. Mackey, “Chaos, fractals and noise”, Vol 97 of Applied Math Science, Springer Verlag (1994), ISBN 0-387-94049-9
- [8] D.C. Champeney, “A handbook of Fourier theorems”, Cambridge University Press (1987), ISBN 0-521-265037.
- [9] J-P. Eckmann and D. Ruelle, *Ergodic theory of chaos and strange attractors*, **Reviews of Modern Physics**, vol. 57 no. 3 part 1, pp 617–656 (1985)
- [10] S.H. Isabelle, *A signal processing framework for the analysis and application of chaotic systems*, **PhD Thesis**, MIT (1995)
- [11] D.C. Hamill and D.J. Jefferies, *Subharmonics and chaos in a controlled switched-mode power converter*, **IEEE Transactions on Circuits and Systems**, vol. 35, no. 8, pp. 1059–1061 (1988).
- [12] L.H. Dixon, *High power factor preregulator for off-line power supplies*, **Unitrode Switching Regulated Supply Design Seminar Manual (SEM-700)**, section I2, Unitrode Corporation (1990)
- [13] S. Banerjee, J.A. Yorke and C. Grebogi, *Robust chaos*, **Physical Review Letters**, (1998, to appear)